ChemPubSoc Europe

DOI: 10.1002/chem.201603600

CHEMISTRY
A European Journal
Full Paper

Computational Chemistry

Influence of Metal, Ligand and Solvent on Supramolecular Polymerizations with Transition-Metal Compounds: A Theoretical Study

Naidel A. M. S. Caturello,[b] Zsolt Csók,[b] and Rodrigo Q. Albuquerque*[a, b]

Abstract: The nature of intermolecular interactions governing supramolecular polymerizations is very important for controlling their cooperativity. In order to address this problem, supramolecular columns made of Pt^{II} and Pd^{II} complexes of oligo(phenylene ethynylene)-based pyridine (OPE) and tetrazolylpyridine ligands (TEP) were investigated through the dispersion-corrected PM6 method. Aromatic, CH–π, M–Cl and metallophilic interactions helped stabilize the supramolecules studied, and their geometries and associated cooperativities were in excellent agreement with experimental data. The OPE ligand and/or the presence of Pt^{II} led to stronger metallophilic interactions and also to cooperative supramolecular polymerizations, which clearly suggests that metallophilic interactions are a key factor for controlling cooperativity. The results indicate that sequential monomer addition is in general less spontaneous than the combination of two larger preformed stacks. The present theoretical investigations contribute to the further understanding of the relation between the thermodynamics of supramolecular polymerizations and the nature of different synthons.

Introduction

Supramolecular polymers[1] consisting of stacked aromatic cores have gained considerable interest in recent times due to their potential in optoelectronic[2] and biomedical applications.[3] Their formation is usually driven by various classes of noncovalent interactions.[4] The most commonly used approach to construct supramolecular self-assembled polymers is the introduction of the conventional hydrogen-bonding motif or the combination of hydrogen-bonding and aromatic interactions.[5–7] The incorporation of metals represented a novel concept in the organization of supramolecular architectures due to the emerging metallophilic interactions, as reported by Fernández et al.[8–11] Furthermore, other weak interactions such as dipole–dipole,[12] C–H···X (X = Cl, O) interactions[10,11] and the hydrophobic effect,[13,14] when combined with aromatic interactions (also known as π–π stacking), can play an important role in the additional stabilization of supramolecular polymeric assemblies.

The cooperativity of supramolecular polymerizations can be rationalized on two main types.[15,16] In the isodesmic process, all growing steps are characterized by the same value of association constant regardless of the sizes of the aggregates. On the contrary, the cooperative mechanism is composed of two separate steps, in which a thermodynamically unfavorable initial nucleation is followed by a highly favored cooperative elongation process characterized by much higher binding constants. As a consequence, cooperative behavior results in longer supramolecular polymers with enhanced degree of internal order and multilevel hierarchy.[17] Cooperativity studies of aggregates based on trisamide derivatives have been described by de Greef and co-workers[18] and by Albuquerque et al.[19] using density functional theory (DFT) and semiempirical calculations, respectively.

Oligo(phenylene ethynylene)s (OPEs) are highly extended, π-conjugated organic molecules, and are well-known for their ability to cooperatively self-assemble into a wide variety of supramolecular structures, driven by noncovalent interactions.[9–11,13,14] It has been also shown that OPEs are able to self-organize into microcrystalline lamellae[20] or into micrometric-size associates[21] as well as to amplify chirality[22] or to invert supramolecular handedness.[23] Furthermore, a recent study confirmed that the interchain π-interactions in OPEs have strong impact on the photophysical properties of the self-assembled materials.[24] Pyridine-centered tridentate ligands are highly versatile building blocks that are extensively used in coordination chemistry.[25] For instance, the combination of a tetrazolylpyridine (TEP) ligand with Pt^{II} led to self-assembled supramolecular nanowires exhibiting aggregation-induced luminescence, as reported by Strassert et al.[26]

The design of new supramolecular polymers of transition-metal complexes with optimal properties for optoelectronic applications requires a fundamental understanding of the mechanism of the self-assembly process. Despite the large

[a] Dr. R. Q. Albuquerque
School of Pharmacy and Biomolecular Sciences
Liverpool John Moores University (LJMU)
Byrom Str. Campus, Liverpool L3 3AF (UK)
E-mail: R.Q.Albuquerque@ljmu.ac.uk

[b] N. A. M. S. Caturello, Dr. Z. Csók, Dr. R. Q. Albuquerque
Sao Carlos Institute of Chemistry
University of Sao Paulo (USP), Sao Carlos (Brazil)

Supporting information for this article can be found under http://dx.doi.org/10.1002/chem.201603600.

© 2016 Wiley-VCH Verlag GmbH & Co. KGaA, Weinheim

These are not the final page numbers! ↗↗

number of experimental work dedicated to supramolecular polymers, there have been only a few computational studies,[18,19,27–29] and in particular, there is only one DFT study involving metal-containing systems.[9]

Herein, we report on a theoretical investigation of four self-assembled metallo-supramolecular columns based either on an OPE pyridine or a TEP ligand (Scheme 1). The roles of the metal and the ligand are evaluated through dipole moments, HOMO–LUMO gaps, intermetallic average distances, and Gibbs energies of formation. Additionally, the general growth mechanisms shown in Scheme 1 are discussed, and the role of the solvent in the stabilization of supramolecular dimers is also investigated.

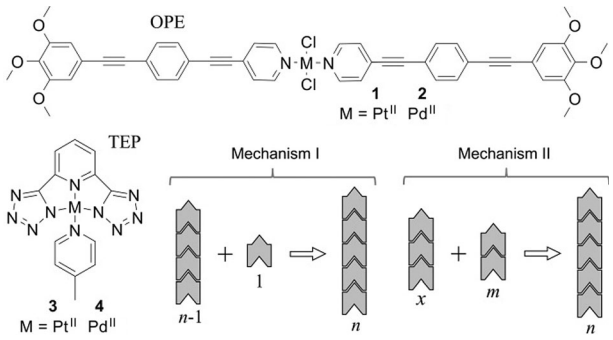

Scheme 1. Structures of the four coordination compounds used as monomers to form supramolecular aggregates and general mechanisms of supramolecular polymerization investigated. The ligands are abbreviated as OPE and TEP.

Results and Discussion

The results shown in this section are based on the semiempirical dispersion-corrected PM6 level of theory, also called PM6-D3H4X,[30] which has been already used to predict the geometry of compounds similar to **1** and **2**.[31] We performed tests with the more recent semiempirical PM7 method,[32] but optimization problems for aggregates as small as dimers were encountered in the case of Pd^{II} complexes, suggesting that this method may not be reliable, at least for the Pd^{II} complexes investigated here. Also, dispersion-corrected PM6 was shown to be superior to PM7 concerning the description of noncovalent interaction.[33] For this reason all calculations reported in the present investigation refer to the PM6-D3H4X model.

The description of the optimized geometries of monomers and aggregates of compounds **1**–**4**, together with the prediction of their aggregation mechanisms, and the discussion of the influence of the metal, the ligand and the solvent on these mechanisms as well as the general properties are shown below.

Optimized geometries and general properties

The optimized geometries of monomers and aggregates formed by compounds **1**–**4** are shown in Figure 1. In general, the columnar shapes of the aggregates predicted from our semiempirical calculations are in good agreement with the experimental results recently published for similar derivatives of **1**–**3**.[9,26,31] The results suggest that **1** and **2** can build aggregates by sequential rotation of each monomer unit by about 13° (for **1**) and 22° (for **2**) with respect to the long axis of the aggregate. This helical structure, which was predicted in vacuum, helps maximize intermolecular interactions within the single supramolecular column. Metal–metal (M–M), aromatic (π–π) and metal–chloride (M–Cl) interactions contributing to the stabilization of the aggregates of **1** and **2** are depicted in the inset of Figure 1. Weak hydrogen bonds involving the side chains also help stabilize the aggregates. Atomic force microscopy (AFM) investigations of aggregates self-assembled from a derivative of **2** bearing long alkyl chains as side groups revealed the presence of such helical structure.[9] Explicit considerations of solvent or intercolumnar interactions present in solid state are expected to influence the final geometry of each single column, but such computationally demanding calculations are out of the scope of this investigation. However, it turns out that vacuum conditions are already good enough to explain not only geometries, but also the cooperativity, as will be discussed later.

The supramolecular aggregates formed by **3** and **4** are very similar and are predicted to be linear, where ligands are sequentially rotated by about 70° with respect to the long axis of the aggregate. The intermolecular aromatic interactions involving pyridine units form a helix, which is highlighted by the long red tubes shown in Figure 1. The same helical disposition occurs with the metallophilic bonds, which together with the pyridine–pyridine interactions give rise to the double helix shown in Figure 1 (transparent tubes). Intermolecular CH–π (pyridine–tetrazole) and aromatic interactions also help stabilize the stack. The interactions involving the pyridines, namely the pyridine–pyridine and CH–π interactions strongly reduce the rotational and vibrational freedom of the pyridine. The predicted vibrational frequency for the out-of-plane deformations of the pyridinic C–H bonds is 2747 cm^{-1} for the monomer and it becomes weaker for the dimer (2726 cm^{-1}) due to the intermolecular CH–π interactions. This might eliminate non-radiative deactivation paths responsible for luminescence quenching, which helps explain why long aggregates of a very similar derivative of **3** undergo aggregation-induced luminescence.[26]

The evolution of some general properties of the aggregates of **1**–**4** upon increasing the number of monomer units *n* is shown in Figure 2. Figure 2a reveals that metallophilic interactions play a crucial role in the stabilization of all aggregates, the corresponding M–M bonds becoming increasingly more stable (or shorter) upon increasing *n*. This means one can interpret Figure 2a as a measure of cooperativity among metal bonds. Note that all intermolecular interactions together contribute to the final thermodynamic quantities governing the aggregation, which may lead to an overall anti-cooperativity as, for instance, predicted for **4** (vide infra), even though the formation of metallophilic bonds can behave cooperatively.

The average metal–metal distance of a decamer predicted from the semiempirical calculations is smaller for **1** (d_{Pt-Pt} = 3.74 Å) than for **2** (d_{Pd-Pd} = 3.85 Å). The comparison between **3**

© 2016 Wiley-VCH Verlag GmbH & Co. KGaA, Weinheim

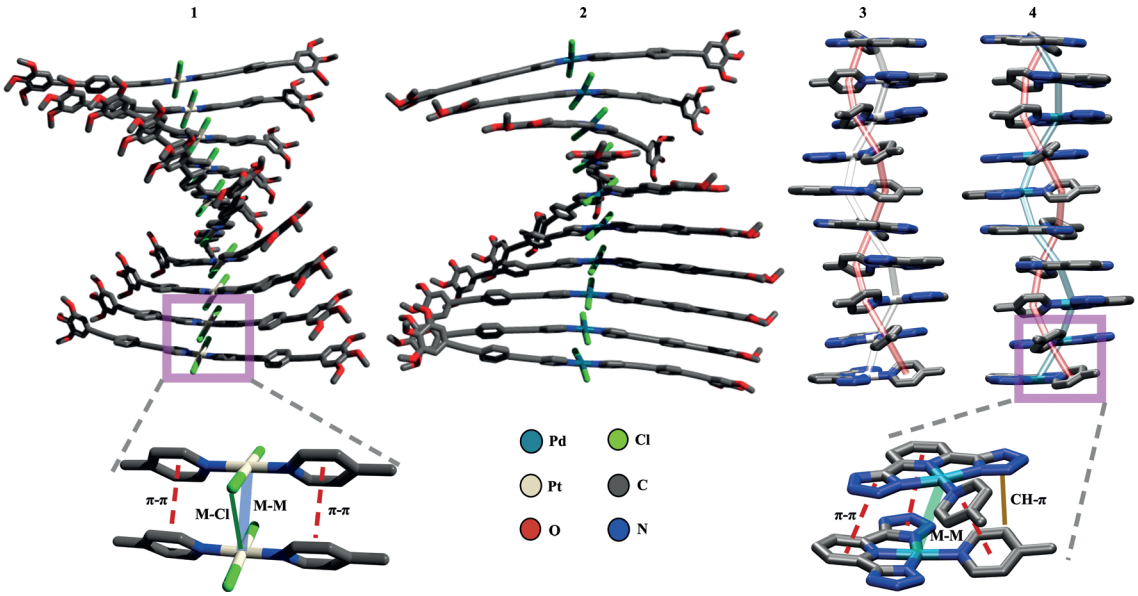

Figure 1. Geometries of decamers of **1**–**4** optimized with the semiempirical PM6-D3H4X method in vacuum. Hydrogen atoms are omitted for clarity. The long tubes (**3** and **4** only) highlight the helical disposition of adjacent pyridines and of metal centers.

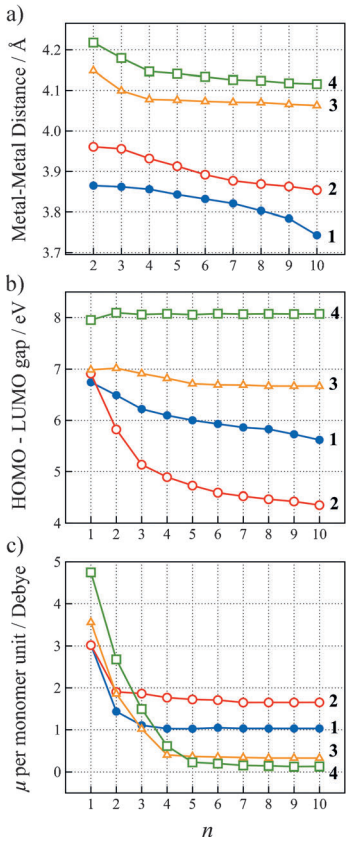

Figure 2. Trends of: a) metal–metal distances, b) HOMO–LUMO gaps, and c) electric dipole moment per monomer unit for aggregates of **1**–**4** with *n* monomer units. Calculations were carried out at the semiempirical PM6-D3H4X level in vacuum.

and **4** (Figure 2a) shows that Pt–Pt bonds are shorter than Pd–Pd ones independently of the ligand. This difference suggests stronger bond strengths for aggregates of **1** and **3**, which is in line with experimental observations of similar supramolecular polymers reported elsewhere.[34] This difference in bond strength is also reflected in the different heats of formation for aggregates of different sizes, which are predominantly more exothermic for Pt^{II}-based aggregates (vide infra).

It may be interesting to see how the nature of the metal and the ligand influence the metal–metal bond strength (Figure 2a). First, if one replaces the OPE ligand (**1** and **2**) by the TEP ligand (**3** and **4**), the metal–metal distance becomes larger, independently of the metal considered. If one keeps the same (TEP) ligand as in **4**, but changes the metal from Pd^{II} to Pt^{II} as in **3**, the metal–metal distance becomes shorter. The same happens when one compares **2** and **1**, where again Pt^{II} gives rise to shorter M–M bond distances. This allows us to conclude that the ligand OPE and/or the presence of Pt^{II} always lead to stronger metallophilic interactions for the systems investigated here.

The HOMO–LUMO gaps decrease upon increasing *n* for the supramolecular systems except for **4**, where it is nearly constant (Figure 2b). A similar red shift of the HOMO–LUMO gap with the increase of *n* has been reported for other supramolecular systems without metal centers and even without aromatic interactions,[19] indicating that the proper arrangement of dipole moments *and* the presence of any strongly stabilizing intermolecular interactions cause that red shift. In the case of **4**, even though the arrangement of dipole moments inside the stack is very similar to that of the aggregates of **3** (Figure 1), the intermolecular interactions do not seem to be strong enough to cause a red shift, which is also evidenced by the larger average metal–metal distance found for **4**. For **1**–**3**, the singlet and triplet excited states are expected to red shift upon increasing the aggregate length, and this has been in fact observed for metal-free supramolecular columns composed of benzene- and cyclohexane-trisamides.[19,35] The aggregates of

© 2016 Wiley-VCH Verlag GmbH & Co. KGaA, Weinheim

1–**3** behave like J-aggregates, as these compounds always show excited states bathochromically shifted with respect to the monomer state. Since the HOMO–LUMO gap is inversely proportional to the polarizability,[19] the trends shown in Figure 2b also reveal that the stacks continuously become softer (or more polarizable) upon growing. This effect is more pronounced for compounds having the OPE ligand (**1** and **2**), and has interesting consequences for the corresponding entropy of aggregation as will be shown.

Figure 2c shows how the total electric dipole moment (μ) per monomer unit changes upon increasing n. The gradual cancellation of individual dipole moments of monomers inside the stacks is observed for all supramolecules. Structures with the OPE ligand (**1** and **2**) always show higher dipole moments. The trend shown in Figure 2c indicates that the geometry of all monomers inside the stack continuously changes upon successive monomer additions up to about $n=10$, and then it tends to be constant. The existence of a cooperative growth for stacks composed of organic trisamide derivatives has been in part associated with a slow increase in the dipole moment per monomer unit.[19] Here, μn^{-1} keeps *decreasing* for all aggregates (this in fact depends on the geometry of each case), but most of them also self-assemble cooperatively, as will be shown later. We will see that other factors, particularly thermodynamic ones, need to be taken into account for attributing positive or negative cooperativity.

Aggregation mechanisms and cooperativity

The changes in enthalpy, entropy, and Gibbs energy for the growth of the supramolecular structures of **1**–**4** following the mechanisms described in Scheme 1 are discussed in this section. The calculated enthalpies ($\Delta_f H$) for the growth of different sizes of aggregates for all compounds and for both assumed mechanisms were always exothermic (Supporting Information, Table S1), as expected, since stabilization is achieved by means of several new intermolecular interactions taking place upon supramolecular aggregation.

The trends obtained for the entropies are worth discussing before exploring the changes in Gibbs energies. The aggregation of the type $m+1 \rightarrow n$ (mechanism I) means that two less organized species are combined to form a more organized supramolecule of n monomer units. One expects intuitively that entropy would decrease, that is, $\Delta_f S < 0$, but the predicted values shown in Figure 3 are not always negative.

If one takes into account only the atomic positions of all the nuclei inside the aggregates and the fact that monomers inside the aggregates have their degrees of freedom restricted, one-dimensional supramolecular aggregates tend to be more organized or less entropic than the precursor monomers. However, supramolecules exhibiting increasingly smaller metal–metal distances, or alternatively, smaller monomer–monomer distances inside a stack tend to delocalize the electrons more along the long axis of the aggregate. Such systems become more polarizable upon growing, as evidenced by the smaller HOMO–LUMO gaps exhibited by larger aggregates (Figure 2b), or even by the red shift of excited states exhibited by other

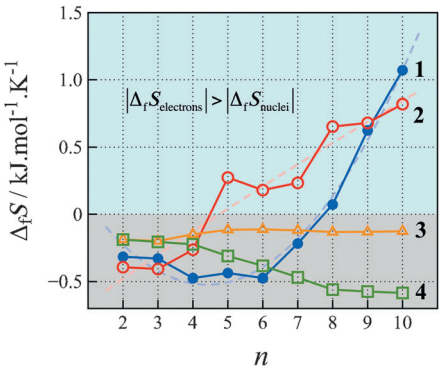

Figure 3. Changes in entropy for the addition of one monomer to a stack of $n-1$ monomers as a function of n for compounds **1**–**4**. Calculations were carried out at the PM6-D3H4X semiempirical level in vacuum at $T=298$ K. The electronic contribution for the entropy, $\Delta_f S_{electrons}$, is dominant at the upper (cyan) part of the plot, while the nuclei contribution, $\Delta_f S_{nuclei}$, is more important at the bottom (gray) part. The dashed lines are trend lines.

1D aggregates.[35] The higher electron delocalization and polarizability lend a higher mobility to the electrons. It becomes then clear that the electronic part of the system, instead of getting more organized and localized, is becoming more disorganized upon self-assembling and therefore $\Delta_f S$ would tend to be more positive. The final $\Delta_f S$ values predicted here (Figure 3) were obtained from molecular partition functions containing both electronic and nuclei contributions, and therefore could be written as: $\Delta_f S = \Delta_f S_{nuclei} + \Delta_f S_{electrons}$. Only for light atoms is the electronic contribution to the partition function negligible because of the very large energy difference between ground and first excited state.[36] For much heavier systems, where excited states or energy levels can become very close to each other,[19,35] the electronic partition function becomes increasingly more important, that is, the degree of accessibility of the electronic states of the system becomes higher.

For aggregates of **1** and **2**, which exhibit considerably smaller HOMO–LUMO gaps and metal–metal distances (Figure 2a and b), the electronic delocalization effects become dominant over the nuclei effects for larger n values and for this reason $\Delta_f S$ gradually increases with n, eventually becoming positive (Figure 3). On the other hand, aggregates of **3** and **4** have larger HOMO–LUMO gaps and metal–metal distances (Figure 2a and b), which means that the electronic delocalization and the polarizability are small. In this case, the increase in entropy caused by the electrons upon supramolecular aggregation is much less pronounced than the decrease in entropy of the nuclei, namely $|\Delta_f S_{nuclei}| > |\Delta_f S_{electrons}|$, and therefore $\Delta_f S < 0$ (Figure 3). In the case of **4**, this is even more extreme, since the large HOMO–LUMO gap (or very small polarizability) is nearly constant (Figure 2b), meaning that the electronic contribution to the entropy becomes much smaller than the one originating from the nuclei; that is, $\Delta_f S$ becomes very negative.

Figure 4 shows how $\Delta_f G$ depends on n for the addition of one monomer to a preformed stack (mechanism I). The supramolecular growth of aggregates of **1**–**3** were predicted to be exergonic ($\Delta_f G < 0$) at room temperature in vacuum and therefore the corresponding stacks are predicted to exist, which is

© 2016 Wiley-VCH Verlag GmbH & Co. KGaA, Weinheim

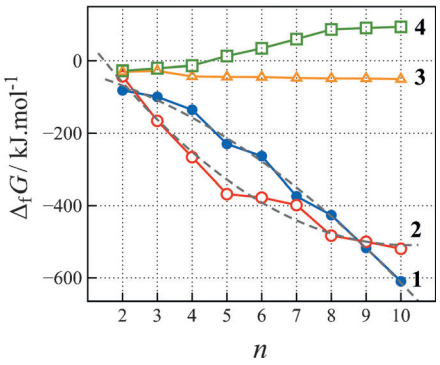

Figure 4. Changes in Gibbs energy for the addition of one monomer to a stack of $n-1$ monomers as a function of n for compounds **1**–**4**. Calculations were carried out at the PM6-D3H4X semiempirical level in vacuum and $\Delta_f G$ was evaluated at $T=298$ K.

in agreement with experimental data of similar compounds.[9,26,31] No experimental data on cooperativity were found for **4**.

According to Figure 4, **1**, **2** and **3** self-assemble cooperatively, that is, the addition of one monomer to a preformed stack makes the next monomer addition even more exergonic. The aggregation of **4** is initially anti-cooperative up to $n=8$, and then it could be regarded as isodesmic, since $\Delta_f G$ becomes approximately constant. The OPE ligand promotes cooperativity independently of the metal, while the TEP derivative does not, which may be related to a greater number of intermolecular interactions present in the OPE-based systems.

The supramolecular growths of **1** and **2** are strongly cooperative, which nicely agrees with the experimental results published elsewhere for similar compounds.[9,31] More importantly, it is evident from Figure 4 that the $\Delta_f G$ curve for **1** is on average steeper than that for **2**, especially if we compare the corresponding trend lines (Figure 4, gray dashed lines). Fernández et al. have recently reported experimental results suggesting that the cooperative self-assembly of a derivative of **1** is considerably stronger than that of a derivative of **2**,[31] which agrees with the results shown in Figure 4. This indicates that the semiempirical calculations reported here are reliable, being able to predict geometries of aggregates, as well as to correctly order the cooperativity of slightly different complexes.

In the theory of nucleation and growth, spontaneous (exergonic) growth can be achieved after a small aggregate or "seed" has been endergonically or non-spontaneously formed. Usually one assumes small seeds ($n\approx2$) in such models, but larger ones can also be adopted.[15] Since endergonic growths were not found for aggregates of **1**–**3**, one may try to interpret the curve obtained for **4** as being part of a large seed, where further growth beyond $n=8$–10 would begin to become cooperative. This assumption is difficult to prove due to the already large number of atoms of the decamer, and because of increasingly higher computational cost, and mainly, convergence problems that would be involved. Temperature effects are also very important to explain the spontaneity of supramolecular aggregations.[9] Semiempirical models are reliable only for room temperature predictions because such models were parameterized to reproduce enthalpies of formation at this temperature. Therefore, direct comparison between the results of the present investigation and the nucleation-and-growth models should be considered with great care, since no kinetic/temperature effects were considered here. Solvation effects may still allow us to qualitatively discuss a bit more of this issue, as will be shown later.

Figure 5 shows how $\Delta_f G$ for the assembling of a supramolecule of n monomer units depends on the sizes of two smaller stacks m and x ($x=2$–5), using **1**–**4** via mechanism II (Scheme 1), where $m+x=n$. For instance, $m+2$ indicates the addition of a preformed stack of m monomer units to a dimer, and it is equivalent to $2+m$. Accordingly, there are four different ways of assembling a decamer, which are represented by four bars at $n=10$: $m+2$ (octamer+dimer), $m+3$ (heptamer+trimer), $m+4$ (hexamer+tetramer), and $m+5$ (pentamer+pentamer). The "$m+1$" case (gray dashed lines) corresponds to the mechanism I and is also shown in Figure 5 for comparison.

According to Figure 5, the most thermodynamically stable supramolecular growth is described by the mechanism II if that growth is cooperative (**1**, **2** and **3**). For instance, it is thermodynamically more stable to grow a pentamer of **1** by combining

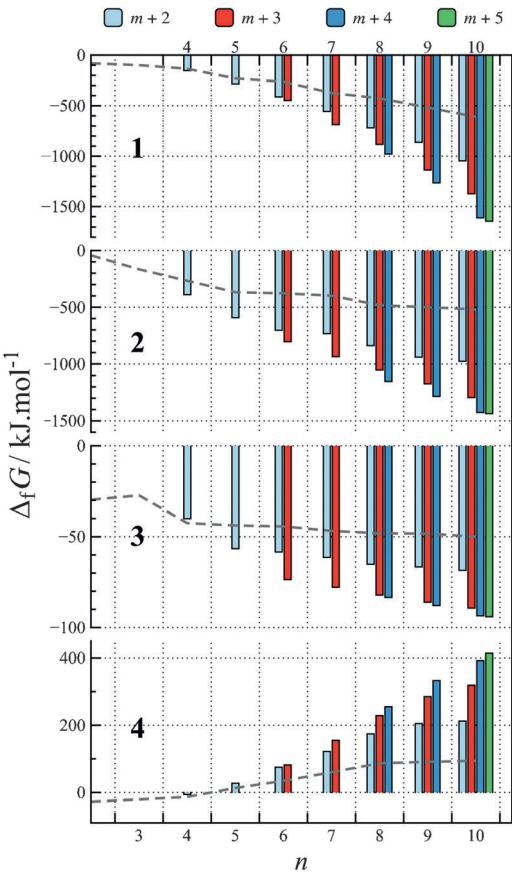

Figure 5. Changes in Gibbs energies for mechanism II (Scheme 1) for the combination of two small stacks of **1**–**4** having m and x ($x=2$–5) monomer units to form a stack of n monomer units ($m+x=n$). Calculations were carried at the PM6-D3H4X semiempirical level in vacuum and $\Delta_f G$ was evaluated at $T=298$ K. Gray dashed lines represent mechanism I for comparison purposes.

© 2016 Wiley-VCH Verlag GmbH & Co. KGaA, Weinheim

a dimer and a trimer (2+3→5) than by adding one monomer on the top of a tetramer (4+1→5). This effect is even more pronounced for larger aggregates: it is twice more exergonic for **1** to build a decamer by combining two pentamers (5+5→10, $\Delta_f H = -860\ kJ\,mol^{-1}$, $\Delta_f S = +2.6\ kJ\,mol^{-1}K^{-1}$) than by combining a nonamer and a monomer (9+1→10, $\Delta_f H = -291\ kJ\,mol^{-1}$, $\Delta_f S = +1.1\ kJ\,mol^{-1}K^{-1}$). This can be understood by paying attention to the respective values of $\Delta_f S$ and $\Delta_f H$. The considerably larger $\Delta_f S$ value predicted for 5+5→10 when compared to 9+1→10 reflects the much larger increase in electronic delocalization and polarizability for the former aggregation, following the same line of previous discussions (vide supra). The $\Delta_f H$ values of 5+5→10 and 9+1→10 are also very different from each other and are related to the fact that, for example, $H_{dimer} \neq 2H_{monomer}$. In other words, the enthalpy per monomer unit (Hn^{-1}) is not constant, but decreases with n as a result of the increasing stabilization inside larger stacks (Figure 6). For instance, for **1** $Hn^{-1} = 498\ kJ\,mol^{-1}$ (monomer) and 411 $kJ\,mol^{-1}$ (dimer). This trend is observed for all compounds, as shown in Figure 6. Figures 3 and 6 are therefore very important for understanding the results shown in Figure 5.

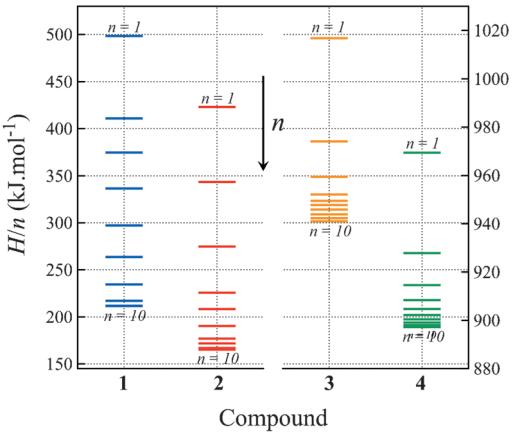

Figure 6. Enthalpy (H) per monomer unit as a function of n for **1**–**4**. Calculations were carried at the PM6-D3H4X semiempirical level in vacuum and H was calculated relative to the elements in their standard state at $T = 298$ K, for which $H \equiv 0$.

Also, it is thermodynamically more stable to combine equally large preformed supramolecular columns ($m \approx x$, for n constant) than preformed stacks of different sizes (Figure 5). For example, building a decamer of **1** becomes increasingly more exergonic in the order 8+2 < 7+3 < 6+4 < 5+5. Finally, if the size of one of the preformed columns is fixed (e.g., dimer = light blue bars in Figure 5), it becomes thermodynamically more spontaneous to grow aggregates by combining it with larger aggregates, as in the sequence 2+2 < 2+3 < 2+4 < ··· < 2+8. Again, Figures 3 and 6 can be used to understand these trends, as already discussed.

Curiously, mechanism I is thermodynamically more stable, that is, the gray dashed line in Figure 5 is more exergonic than the bars, for aggregates of **4**, which are predicted to grow *anti-cooperatively*. This can be explained by the smaller electronic contributions to the partition function exhibited by **4**. Aggregates of **4** have increasingly negative $\Delta_f S$ as a result of the condition $|\Delta_f S_{nuclei}| \gg |\Delta_f S_{electrons}|$ (vide supra), which strongly influences $\Delta_f G$. We can compare 9+1→10 (mechanism I, $\Delta_f H = -80\ kJ\,mol^{-1}$) and 5+5→10 (mechanism II, $\Delta_f H = -76\ kJ\,mol^{-1}$). Since the entropy of the decamer is much smaller than that of the pentamers due to electronic effects, the latter aggregation has $\Delta_f S = -1.64\ kJ\,mol^{-1}K^{-1}$, while for the former $\Delta_f S = -0.58\ kJ\,mol^{-1}K^{-1}$ (the entropies of a nonamer and decamer are much more similar). For these two aggregations, one $\Delta_f S$ is almost three times more negative than the other, while the corresponding $\Delta_f H$ values are basically the same. At 298 K, the very negative value of $\Delta_f S$ found for 5+5→10 is considerably more important than the enthalpic factors ($|T\Delta_f S_{nuclei}| \gg |\Delta_f H|$), and as a consequence, this process is very endergonic ($\Delta_f G = +414\ kJ\,mol^{-1}$). For 9+1→10 the entropic factors still overcompensate the enthalpic ones, but to a lesser extent, and the self-assembly becomes less endergonic ($\Delta_f G = +94\ kJ\,mol^{-1}$).

It is important to recognize the limitation of the results shown in Figure 5. In terms of the total probability for the formation of a supramolecule, kinetic factors should also be taken into account, as already discussed (vide supra). For instance, 5+5 is much more thermodynamically favorable than 9+1 for **1**, **2**, and **3** (and exactly the opposite for **4**). This only reflects thermodynamic parameters, since a preformed pentamer would diffuse much more slowly than a monomer in solution. The monomer would then find a nonamer and get the right spatial orientation for a much faster self-assembly than two pentamers would do, even though 5+5 is predicted to be more exergonic.

Solvent effects

Although the addition of solvent to the large structures simulated in this work led to convergence problems most likely due to a very shallow potential energy surface, such calculations were carried out at least for monomers and dimers by using the nonpolar methylcyclohexane (MCH) solvent. The approach used here was to explicitly add a layer of solvent and to treat the whole system (solute+solvent) by the COSMO model,[37] which uses an implicit solvent layer represented by a continuous dielectric medium. The final optimized dimer structures of **1**–**4** are shown in Figure 7, together with the variations in Gibbs energy for the dimerization process. In all cases, the dimerizations became endergonic, in contrast to the corresponding dimerizations obtained in vacuum (Figure 4). While aromatic interactions are still observed in the solvated dimer, metal–metal distances become on average 0.1 Å longer for all dimers, and therefore slightly weaker when compared with vacuum conditions. The results suggest that, at least for the MCH solvent, dimerization is not spontaneous, which in principle agrees with the nucleation-and-growth models, where a small seed is first endergonically formed, followed by an exergonic elongation step.

© 2016 Wiley-VCH Verlag GmbH & Co. KGaA, Weinheim

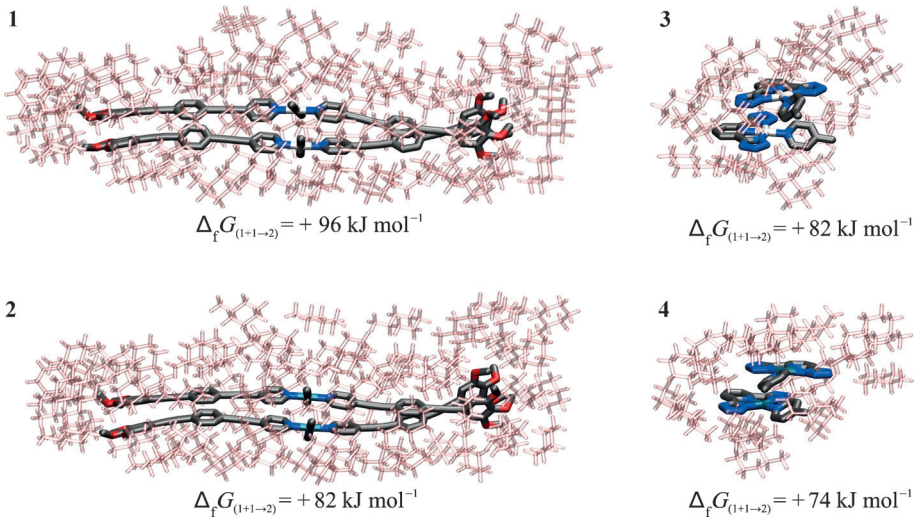

Figure 7. Optimized geometry of dimers of **1**–**4** solvated by MCH and treated by using the implicit-solvent COSMO model. Solute hydrogen atoms were omitted for clarity. Calculations were carried out at the PM6-D3H4X level, and the shown dimerization $\Delta_f G$ values were evaluated at 298 K.

If we suppose that MCH only shifts up the whole $\Delta_f G$ curves shown in Figure 4 as it did with the dimerization $\Delta_f G$ values, one may adopt the endergonic dimerization values shown in Figure 7 to make an extrapolation inside Figure 4 to finally find that the growth in MCH would become exergonic from $n = 5$ for **1**, $n = 3$ for **2**, and $n > 30$ for **3**. For compound **4**, a solvent other than MCH with a higher polarity should be used to achieve an exergonic growth. In these cases the corresponding seeds would be one monomer unit smaller than those extrapolated n values. This is, of course, a very rough picture of the whole self-assembly process, since full consideration of many solvent layers for all sizes of aggregates of **1**–**4** should be taken, which is still very challenging.

Conclusions

We have investigated two different mechanisms of supramolecular polymerization for transition-metal complexes, and discussed the roles of the metal, the ligand and the solvent on thermodynamical aspects and the cooperativity of such processes. The geometries predicted for the aggregates of **1**–**3** nicely agreed with experimental measurements carried out for similar compounds, and in particular, the helical structure predicted for a decamer of **2** has closely matched previous AFM results. Several intermolecular interactions were responsible for the stabilization of the supramolecular systems, namely aromatic, CH–π, M–Cl and metallophilic (M–M) interactions, the latter playing a very important role on the cooperativity of supramolecular polymerizations. The calculations have revealed that the intermolecular aromatic and CH–π interactions present in the aggregates of **3** are responsible for the loss of mobility (rotation and vibration) of the pyridines, which may explain why similar compounds do exhibit aggregation-induced luminescence.

The semiempirical calculations have suggested that mechanism II is thermodynamically preferred over mechanism I for **1**–**3**, that is, the sequential monomer addition is less spontaneous than the combination of two larger preformed stacks. We have predicted positive cooperativity for the supramolecular growth of **1**–**3**, and that the aggregation of **1** is considerably more cooperative than that of **2**, which is in excellent agreement with experimental results. The ligand OPE and/or the presence of Pt^{II} have led to stronger metallophilic interactions and also to cooperative supramolecular polymerizations, which clearly suggest that the presence of metallophilic interactions is a key factor for controlling cooperativity.

The more pronounced electron delocalization and polarizability predicted for aggregates of **1** and **2**, as evidenced from the small HOMO–LUMO gaps and shorter M–M distances, have been related to the non-negligible electronic contribution to the molecular partition function, which was responsible for the strongly positive $\Delta_f S$ predicted for the corresponding supramolecular polymerizations.

The addition of explicit and implicit solvent layers has indicated that dimerizations are endergonic in MCH, and has also enabled us to make a rough estimation of the size n of the seed for aggregates of **1** ($n = 4$) and **2** ($n = 2$), which may be interpreted in terms of the nucleation-and-growth model.

The semiempirical dispersion-corrected PM6 method has proven to be appropriate for describing not only the thermodynamics of all aggregates, but also their geometries and intermolecular interactions. The theoretical investigations described here will contribute to the further understanding of supramolecular polymerizations and to the design of novel supramolecular systems based on the relation between their thermodynamics and the nature of existing synthons.

© 2016 Wiley-VCH Verlag GmbH & Co. KGaA, Weinheim

Experimental Section

Investigated systems

The coordination compounds **1**–**4** shown in Scheme 1 were chosen for this work because of the availability of experimental data describing the formation of supramolecular systems with some of their derivatives. Ligands bearing OPE (**1** and **2**) and TEP (**3** and **4**) moieties were used. For instance, replacing the methyl group of the side chains of **1** and **2** by long glycol and alkyl groups led to compounds able to form supramolecular stackings.[9,11,31] A closely related compound to **3** was reported by Strassert et al. to form supramolecular nanowires exhibiting interesting photophysical properties.[26] The other compound was included in this series in order to allow for investigating the influence of the central metal on the assembling and final properties of the supramolecular stackings. The 1D supramolecular structures of compounds **1**–**4** were then built with *n* monomer units ($n = 1$–10) and their properties investigated.

Calculation of properties

The geometry of the 1D supramolecular polymers built from compounds **1**–**4** with different *n* values ($n = 1$–10) were fully optimized by performing semiempirical calculations using the PM6-D3H4X Hamiltonian[30] as implemented in the MOPAC2012 program suite.[38] This method explicitly takes into account hydrogen bonds and other dispersion interactions, which are of fundamental importance in the formation of self-assembled supramolecular polymers. To take into account the interactions with methylcyclohexane (MCH), monomers and dimers were first solvated with one layer of MCH, then the whole system (solute+solvent) was surrounded by a dielectric layer through the COSMO model.[37] Vibrational frequencies were also calculated for all stacks to check the reliability of the geometry optimizations by the absence of negative frequencies.

General mechanisms of aggregation

In the present study, two different supramolecular aggregation mechanisms were investigated, which are shown in Scheme 1. Mechanism I involves sequential steps in which one monomer unit is added to the former supramolecular column to form the final aggregate.[15] This mechanism is widely used in studies of cooperativity of 1D stackings.[9,31] In mechanism II, an aggregate of *n* monomers is assembled from two smaller columns of *m* and *x* monomer units. The variation in Gibbs energy ($\Delta_f G$) associated to each mechanistic step was calculated in the usual way, for example, $\Delta_f G_{(7+1\rightarrow 8)} = \Delta_f H_{(7+1\rightarrow 8)} - T\Delta_f S_{(7+1\rightarrow 8)}$, where $\Delta_f H_{(7+1\rightarrow 8)} = \Delta_f H_{(8)} - \Delta_f H_{(7)} - \Delta_f H_{(1)}$, and $\Delta_f S_{(7+1\rightarrow 8)} = \Delta_f S_{(8)} - \Delta_f S_{(7)} - \Delta_f S_{(1)}$. For each aggregate, the quantities $\Delta_f H_{(x)}$ and $\Delta_f S_{(x)}$ were calculated relative to the elements in their standard state. The heats of formation at 298 K were directly obtained in the output of the MOPAC program for the geometry optimization step. For the entropy at 298 K, a thermodynamic calculation based on the molecular partition function was carried out by using the same program with the keyword "thermo".

Acknowledgements

The authors would like to acknowledge the LJMU and Brazilian agencies CNPq (400112/2014–0), CAPES (A061_2013) and FAPESP (2014/02071-5) for financial support.

Keywords: cooperativity · self-assembly · semiempirical calculations · supramolecular polymerization · transition-metal complexes

[1] T. F. A. de Greef, M. M. J. Smulders, M. Wolffs, A. P. H. J. Schenning, R. P. Sijbesma, E. W. Meijer, *Chem. Rev.* **2009**, *109*, 5687 – 5754.
[2] J. D. Tovar, *Acc. Chem. Res.* **2013**, *46*, 1527 – 1537.
[3] S. Cantekin, T. F. A. de Greef, A. R. A. Palmans, *Chem. Soc. Rev.* **2012**, *41*, 6125 – 6137.
[4] C. Rest, R. Kandanelli, G. Fernandez, *Chem. Soc. Rev.* **2015**, *44*, 2543 – 2572.
[5] P. Jonkheijm, P. van der Schoot, A. P. H. J. Schenning, E. W. Meijer, *Science* **2006**, *313*, 80 – 83.
[6] P. A. Korevaar, S. J. George, A. J. Markvoort, M. M. J. Smulders, P. A. Hilbers, A. P. H. J. Schenning, T. F. A. de Greef, E. W. Meijer, *Nature* **2012**, *481*, 492 – 496.
[7] T. Mes, S. Cantekin, D. W. R. Balkenende, M. M. M. Frissen, M. A. J. Gillissen, B. F. M. De Waal, I. K. Voets, E. W. Meijer, A. R. A. Palmans, *Chem. Eur. J.* **2013**, *19*, 8642 – 8649.
[8] M. J. Mayoral Muñoz, G. Fernández, *Chem. Sci.* **2012**, *3*, 1395 – 1398.
[9] M. J. Mayoral, C. Rest, V. Stepanenko, J. Schellheimer, R. Q. Albuquerque, G. Fernández, *J. Am. Chem. Soc.* **2013**, *135*, 2148 – 2151.
[10] C. Rest, A. Martin, V. Stepanenko, N. K. Allampally, D. Schmidt, G. Fernández, *Chem. Commun.* **2014**, *50*, 13366 – 13369.
[11] C. Rest, M. J. Mayoral, K. Fucke, J. Schellheimer, V. Stepanenko, G. Fernández, *Angew. Chem. Int. Ed.* **2014**, *53*, 700 – 705; *Angew. Chem.* **2014**, *126*, 716 – 722.
[12] G. Fernández, M. Stolte, V. Stepanenko, F. Würthner, *Chem. Eur. J.* **2013**, *19*, 206 – 217.
[13] M. J. Mayoral, C. Rest, J. Schellheimer, V. Stepanenko, G. Fernández, *Chem. Eur. J.* **2012**, *18*, 15607 – 15611.
[14] N. K. Allampally, A. Florian, M. J. Mayoral, C. Rest, V. Stepanenko, G. Fernández, *Chem. Eur. J.* **2014**, *20*, 10669 – 10678.
[15] D. Zhao, J. S. Moore, *Org. Biomol. Chem.* **2003**, *1*, 3471 – 3491.
[16] C. Kulkarni, S. Balasubramanian, S. J. George, *ChemPhysChem* **2013**, *14*, 661 – 673.
[17] T. Aida, E. W. Meijer, S. Stupp, *Science* **2012**, *335*, 813 – 817.
[18] I. A. W. Filot, A. R. A. Palmans, P. A. J. Hilbers, R. A. van Santen, E. A. Pidko, T. F. A. de Greef, *J. Phys. Chem. B* **2010**, *114*, 13667 – 13674.
[19] R. Q. Albuquerque, A. Timme, R. Kress, J. Senker, H.-W. Schmidt, *Chem. Eur. J.* **2013**, *19*, 1647 – 1657.
[20] G. Fernández, F. García, F. Aparicio, E. Matesanz, L. Sánchez, *Chem. Commun.* **2009**, 7155 – 7157.
[21] A. Florian, M. J. Mayoral, V. Stepanenko, G. Fernández, *Chem. Eur. J.* **2012**, *18*, 14957 – 14961.
[22] F. García, L. Sánchez, *J. Am. Chem. Soc.* **2012**, *134*, 734 – 742.
[23] A. Gopal, M. Hifsudheen, S. Furumi, M. Takeuchi, A. Ajayaghosh, *Angew. Chem. Int. Ed.* **2012**, *51*, 10505 – 10509; *Angew. Chem.* **2012**, *124*, 10657 – 10661.
[24] S. P. Jagtap, S. Mukhopadhyay, V. Coropceanu, G. L. Brizius, J.-L. Brédas, D. M. Collard, *J. Am. Chem. Soc.* **2012**, *134*, 7176 – 7185.
[25] J. P. Byrne, J. A. Kitchen, T. Gunnlaugsson, *Chem. Soc. Rev.* **2014**, *43*, 5302 – 5325.
[26] C. A. Strassert, C.-H. Chien, M. D. Galvez Lopez, D. Kourkoulos, D. Hertel, K. Meerholz, L. De Cola, *Angew. Chem. Int. Ed.* **2011**, *50*, 946 – 950; *Angew. Chem.* **2011**, *123*, 976 – 980.
[27] K. K. Bejagam, G. Fiorin, M. L. Klein, S. Balasubramanian, *J. Phys. Chem. B* **2014**, *118*, 5218 – 5228.
[28] K. K. Bejagam, S. Balasubramanian, *J. Phys. Chem. B* **2015**, *119*, 5738 – 5746.
[29] K. K. Bejagam, C. Kulkarni, S. J. George, S. Balasubramanian, *Chem. Commun.* **2015**, *51*, 16049 – 16052.
[30] J. Řezáč, P. Hobza, *J. Chem. Theory Comput.* **2012**, *8*, 141 – 151.
[31] N. K. Allampally, M. J. Mayoral, S. Chansai, M. C. Lagunas, C. Hardacre, V. Stepanenko, R. Q. Albuquerque, G. Fernández, *Chem. Eur. J.* **2016**, *22*, 7810 – 7816.
[32] J. J. P. Stewart, *J. Mol. Model.* **2013**, *19*, 1 – 32.
[33] J. Hostaš, J. Řezáč, P. Hobza, *Chem. Phys. Lett.* **2013**, *568 – 569*, 161 – 166.

© 2016 Wiley-VCH Verlag GmbH & Co. KGaA, Weinheim

[34] M. Chen, C. Wei, J. Tao, X. Wu, N. Huang, G. Zhang, L. Li, *Chem. Eur. J.* **2014**, *20*, 2812 – 2818.
[35] A. Bernet, R. Q. Albuquerque, M. Behr, S. T. Hoffmann, H.-W. Schmidt, *Soft Matter* **2012**, *8*, 66 – 69.
[36] D. A. McQuarrie, in *Statistical Thermodynamics*, University Science Books, Mill Valley, **1973**.
[37] A. Klamt, G. Schürrmann, *J. Chem. Soc. Perkin Trans. 2* **1993**, 799 – 805.
[38] a) MOPAC2012, J. P. Stewart, Computational Chemistry, Version 15.180m, http://openmopac.net; b) J. D. C. Maia, G. A. U. Carvalho, Jr., C. P. Mangueira, S. R. Santana, L. A. F. Cabral, G. B. Rocha, *J. Chem. Theory Comput*. **2012**, *8*, 3072 – 3081.

Received: July 28, 2016
Published online on ■■ ■■, 0000

© 2016 Wiley-VCH Verlag GmbH & Co. KGaA, Weinheim

FULL PAPER

Computational Chemistry

*N. A. M. S. Caturello, Z. Csók, R. Q. Albuquerque**

■■ – ■■

Influence of Metal, Ligand and Solvent on Supramolecular Polymerizations with Transition-Metal Compounds: A Theoretical Study

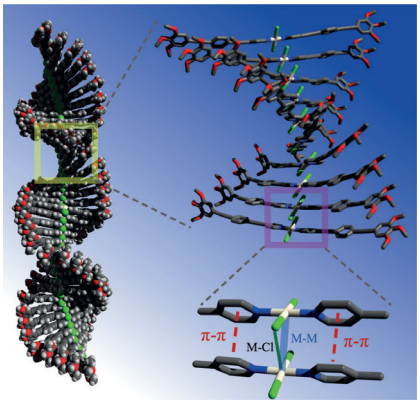

Cooperative × anti-cooperative: How can interactions involving different metals and ligands be used to predict cooperativity for the self-assembly of large supramolecular architectures? To address this problem, supramolecular columns made of Pt^{II} and Pd^{II} complexes of oligo(phenylene ethynylene)-based pyridine and tetrazolylpyridine ligands (see figure) were investigated through the dispersion-corrected PM6 method.

© 2016 Wiley-VCH Verlag GmbH & Co. KGaA, Weinheim